

Ballistic Hot Electron Transport in Graphene

Wang-Kong Tse, E. H. Hwang, and S. Das Sarma
*Condensed Matter Theory Center, Department of Physics,
 University of Maryland, College Park, Maryland 20742-4111, USA*

We theoretically study the inelastic scattering rate and the carrier mean free path for energetic hot electrons in graphene, including both electron-electron and electron-phonon interactions. Taking account of optical phonon emission and electron-electron scattering, we find that the inelastic scattering time $\tau \sim 10^{-2} - 10^{-1}$ ps and the mean free path $l \sim 10 - 10^2$ nm for electron densities $n = 10^{12} - 10^{13} \text{ cm}^{-2}$. In particular, we find that the mean free path exhibits a finite jump at the phonon energy 200 meV due to electron-phonon interaction. Our results are directly applicable to device structures where ballistic transport is relevant with inelastic scattering dominating over elastic scattering.

The existence [1] of gated two-dimensional (2D) graphene layers, where carrier transport controlled by an external gate has become possible [2], provides the exciting possibility of novel high-speed electronic device structures [3] utilizing the high graphene carrier mobility [2, 4]. Such fast graphene devices would work in the ballistic transport regime, where carrier mobility limited by elastic scattering, is essentially irrelevant (i.e. $l_e > l$, with l_e , l , being respectively the elastic and the inelastic carrier mean free path), and what matters is the inelastic scattering due to electron-electron and electron-phonon interactions. Such ballistic devices for ultrafast applications can only work if the relevant device dimensions are smaller than the inelastic mean free path l , and the speed of this device is limited by the inelastic scattering time τ ($< \tau_e$, where τ_e is the elastic relaxation time). In currently available high-mobility ($> 20,000 \text{ cm}^2/\text{Vs}$) graphene samples, $l_e(\tau_e) \gtrsim 10^3 \text{ nm}$ (1 ps), and therefore, inelastic scattering will dominate device operations for length (time) scales below 10^3 nm (1 ps).

In this Letter, we calculate the inelastic mean free path (l) and the corresponding inelastic scattering rate τ^{-1} in graphene limited by electron-electron and electron-phonon interactions. Our study is motivated by electron transport in the hot electron transistor device structure which is so designed as to allow electrons to traverse the base region ballistically. In such a device scheme, highly energetic electrons are injected in the emitter region which then travel through the base region ballistically before reaching the collector region. The fraction of electrons α that reach the collector goes as $\alpha \sim e^{-d/l}$, where d is the width of the base region. The mean free path is given by $l = v\tau$, where v is the Fermi velocity of electron and τ is the inelastic scattering time, which, in general, is a strong function of the injected energy of electrons and the electron density in the base region.

We consider two principal mechanisms contributing to inelastic scattering arising from many-body interactions: (1) absorption or emission of optical phonons by electrons due to electron-phonon (e-ph) interaction; (2) exchange-correlation effects induced by electron-electron (e-e) interaction. For the e-ph interaction, we take into account the most dominant phonon mode in graphene – the LO

phonons at the Brillouin zone center Γ . This mode shows up as the ‘G peak’ resonance observed in Raman scattering experiments with a phonon energy $\omega_0 \approx 200 \text{ meV}$ [5]. Acoustic phonons couple very weakly to electrons in graphene, and the associated scattering rates are on the order of 10^{11} s^{-1} even at room temperature [6] and can be ignored when compared to the scattering mechanism discussed above. We also neglect electron-impurity scattering in our calculation because the mean free paths of currently available high mobility graphene samples are much longer than the inelastic mean free paths to be calculated in this paper.

The inelastic scattering of electrons causes damping (i.e., decay) of the quasiparticle state, and the inelastic scattering lifetime $\tau(k)$ is given by the imaginary part of the self-energy $\text{Im}\Sigma(k, E)$ evaluated on the energy shell $E = \xi_k$, where $\xi_k = \varepsilon_k - \mu$ ($\varepsilon_k = \hbar vk$ is the electron kinetic energy and $v \approx 10^6 \text{ ms}^{-1}$ is the Fermi velocity which is constant in graphene irrespective of electron density) is the single-particle energy rendered from the chemical potential μ . The inelastic scattering rate (or damping rate) $1/\tau$ consists of two contributions, given by $\hbar/2\tau(k) = \text{Im}\Sigma_{\text{e-ph}}^{\text{R}}(k, \xi_k) + \text{Im}\Sigma_{\text{e-e}}^{\text{R}}(k, \xi_k)$, where the first term denotes the contribution to the self-energy due to electron-LO phonon interaction [7],

$$\text{Im}\Sigma_{\text{e-ph}}^{\text{R}}(k, \xi_k) = -\pi g^2 \sum_{\lambda=\pm 1} \sum_{k'} \{n_F(\xi_{k'\lambda}) \delta(\xi_k - \xi_{k'\lambda} + \omega_0) + [1 - n_F(\xi_{k'\lambda})] \delta(\xi_k - \xi_{k'\lambda} - \omega_0)\} \frac{1 - \lambda \cos(\phi_{k'} - 2\phi_{k-k})}{2}, \quad (1)$$

and the second term on the right denotes the contribution to the self-energy due to e-e Coulomb interaction [8],

$$\text{Im}\Sigma_{\text{e-e}}^{\text{R}}(k, \xi_k) = \sum_{\lambda=\pm 1} \sum_{k'} [n_B(\xi_{k'\lambda} - \xi_k) + n_F(\xi_{k'\lambda})] V_{\mathbf{k}'-\mathbf{k}} \text{Im} \left[\frac{1}{\epsilon(\mathbf{k}' - \mathbf{k}, \xi_{k'\lambda} - \xi_k + i0^+)} \right] \frac{1 + \lambda \cos(\phi_{k'} - \phi_k)}{2}. \quad (2)$$

Here, $n_B(x), n_F(x) = 1/(\exp(x/k_B T) \mp 1)$ are the Bose and Fermi distribution functions, respectively. For the e-ph contribution Eq. (1), $g = -(\beta \hbar v/a^2) \sqrt{(\hbar/2NM_c \omega_0)}$

is the e-ph coupling constant [9], where $\beta \simeq 2$ is a dimensionless constant characterizing the rate of change of the nearest-neighbor hopping energy with respect to bond length, $a = 1.42 \text{ \AA}$ is the equilibrium bond length, N is the number of unit cells, $M_C = 2.2 \times 10^4 m_e$ is the mass of a carbon atom (m_e is the electron mass). For the Coulomb contribution Eq. (2), $V_q = 2\pi e^2/q$ is the bare Coulomb interaction, $\epsilon(q, \omega) = 1 - V_q \Pi(q, \omega)$ is the dielectric function given, within the random phase approximation, by the electron polarizability $\Pi(q, \omega)$ [10].

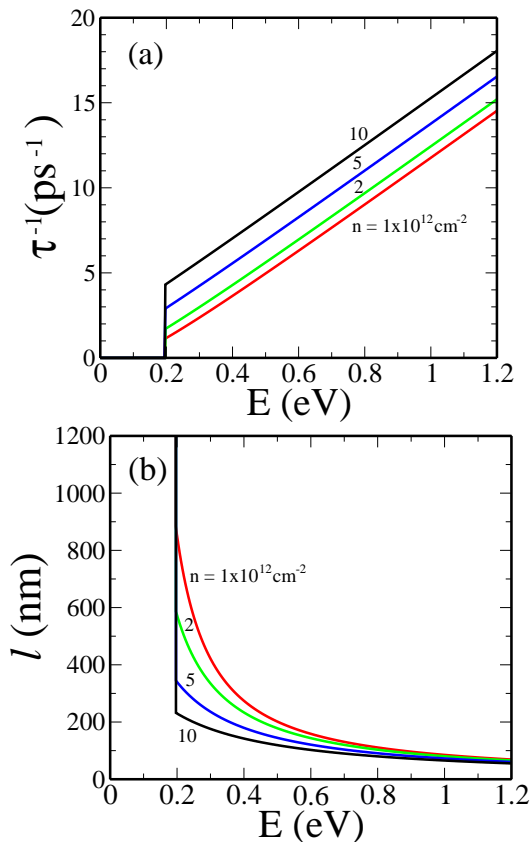


FIG. 1: (a) Inelastic scattering rate due to e-ph interaction versus the single-particle energy of hot electron $E = \xi_k$ for different electron densities n . $n = 1, 2, 5, 10 \times 10^{12} \text{ cm}^{-2}$ are indicated by the red, green, blue and black lines, respectively. (b) Corresponding inelastic mean free path l .

In the following, we calculate $1/\tau(k)$ at zero temperature, which is a very good approximation for graphene since at the usual doping density $n = 10^{12} - 10^{13} \text{ cm}^{-2}$, the corresponding Fermi temperature $T_F \simeq 1400 - 4300 \text{ K}$ is much higher than room temperature. First we calculate the self-energy correction due to e-ph interaction, Eq. (1). Fig. 1(a) shows the scattering rate $1/\tau$ versus electron energy $E = \xi_k$ for different values of electron density. The gap from 0 to 0.2 eV (which is the LO phonon energy ω_0) is a characteristic feature of the LO phonon absorption process; it results from the Pauli blocking by those electrons located within an amount

of energy ω_0 of the Fermi level, so that decay by electrons with energy $\xi_k \in [-\omega_0, \omega_0]$ is forbidden due to the restricted phase space. Beyond the gap, $1/\tau$ behaves linearly as k due to the linear dependence on momentum of the graphene density of states, $\nu(k) = 2k/\pi\hbar v$. As a result of the gap in $1/\tau$, the calculated mean free path $l = v\tau$ [Fig. 1(b)] is infinite within the range of the phonon energies, before falling off as $\sim 1/E$ with electron energy E . Fig. 1 also shows that the scattering rate (mean free path) increases (decreases) with electron density, as scattering events become more frequent with increasing number of electrons.

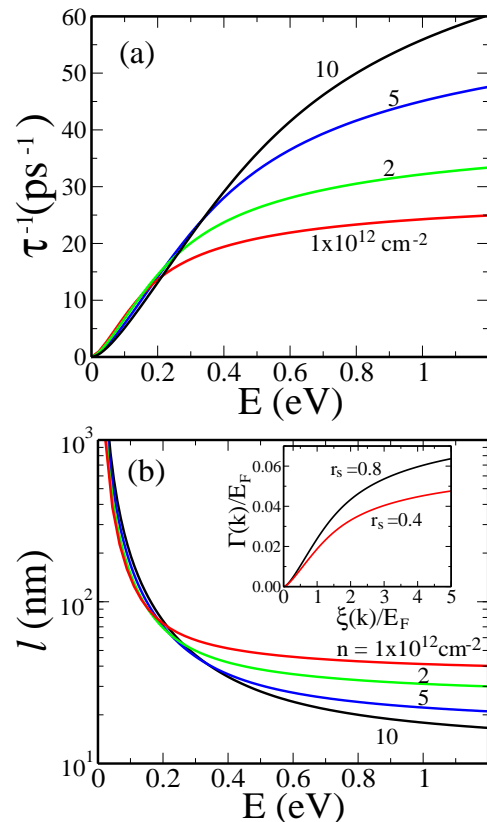


FIG. 2: Calculated scattering rate (a) and the corresponding mean free path (b) of hot carrier electron as a function of energy $E = \xi_k$ for different carrier densities $n = 1, 2, 5, 10 \times 10^{12} \text{ cm}^{-2}$. The inset in (b) shows the calculated damping rate $\Gamma(k) \equiv \hbar/2\tau(k)$ scaled by Fermi energy as a function of energy divided by Fermi energy for different coupling constant $r_s = 0.8$ and 0.4 , which correspond to graphene on SiO_2 and SiC substrates, respectively. Note the scaled damping rates are independent on the density.

For e-e Coulomb interaction, we show the calculated inelastic scattering rate Eq. (2) and the corresponding inelastic mean free path, $l = v\tau$ in Fig. 2. The strength of Coulomb interaction is characterized by the dimensionless coupling parameter $r_s = e^2/\kappa\hbar v$, where κ is the effective background dielectric constant of the substrate [10]. In the inset of Fig. 2(b), the calculated damping rates are shown for different coupling constants $r_s = 0.8$

and $r_s = 0.4$. Before discussing the scattering time we consider the scattering rate $1/\tau$ due to the e-e interaction. In conventional parabolic-band semiconductors, an electron injected with sufficient kinetic energy can decay via both plasmon emissions and single-particle intraband excitations (i.e. Landau damping) [11]. In doped graphene, however, injected electrons cannot decay via plasmon emission due to phase space restrictions [12]. Multiparticle excitations, which are excluded in the approximations used here, will constitute finite damping of the quasiparticles, but the effects of such higher-order processes are relatively small in graphene. (Note that in undoped graphene even single-particle excitations are forbidden, so that the scattering rate within the Born approximation is zero due to electron-electron Coulomb interaction at $T = 0$ [8].) Since only single-particle excitations give rise to damping of the quasiparticles, for electron energy close to the Fermi level the calculated scattering rate due to e-e interaction in graphene, similar to the case of 2D parabolic-band semiconductors, is given by $1/\tau \sim |\varepsilon_k - E_F|^2 \ln|\varepsilon_k - E_F|$ [8, 12]. Farther away from E_F , however, the dependences of $1/\tau(k)$ on k in graphene and in parabolic-band semiconductors are *qualitatively* different because both plasmon emissions and interband processes are absent in graphene. On the other hand, the only independent parameters relevant for the quasiparticle scattering rate under the Born approximation at $T = 0$ are the Fermi energy and the dimensionless coupling constant r_s . Therefore the calculated scattering rate due to e-e interaction, which has units of energy, must be proportional to E_F , and must be a function only of $\varepsilon_k/E_F = k/k_F$ and r_s [see the inset of Fig. 2(b)].

In Fig. 2(a) the inverse lifetime in units of inverse of ps is shown as a function of energy $E = \xi_k$ of the hot electrons. Below 200 meV, which corresponds to the optical phonon energy of graphene, the calculated scattering time is only weakly dependent on the carrier density of the system. However, for very energetic hot electron $E \gtrsim 1\text{eV}$ the scattering time shows a strong density dependence and increases by almost a factor of two as the density decreases from $n = 10^{13} \text{ cm}^{-2}$ to $n = 10^{12} \text{ cm}^{-2}$. Our results are consistent with recent experiments of decay time in ultrafast carrier [13], in which the measured

decay times are in the 0.07 – 0.12 ps range. The corresponding inelastic mean free path is shown in Fig. 2(b) as a function of energy. We find that the characteristic mean free path of the hot electron with 100 meV energy above the Fermi energy is about 100 nm. Again below 200 meV the calculated mean free path is weakly dependent on density.

Combining the results from the e-ph (Fig. 1) and e-e interactions (Fig. 2), the total scattering rate becomes non-zero below the phonon energy 200 meV, and the mean free path $l \sim 10 - 10^2 \text{ nm}$ for injected energy $E < 200 \text{ meV}$ whereas $l \sim 10 \text{ nm}$ for $E > 200 \text{ meV}$.

We now propose an interesting device principle based on our results in this paper, which are peculiar to the many-body effects in graphene. In doped (or gated) graphene, the dominant inelastic scattering process of hot electrons below 200 meV comes from intraband single-particle excitation due to screened electron-electron interaction; above 200 meV, inelastic scattering due to e-ph interaction sets in as electrons are now able to emit LO phonons. A lateral hot-electron transistor (LHET) device [14] where the electrons travel in the graphene sheet of the base region can in principle be fabricated, whose operation makes use of the abrupt change in the inelastic mean free path due to electron-coupled mode scatterings of the injected electrons. Thus, by varying the inelastic scattering rate through changing the injection energy, one can achieve a significant change in the electron mean free path and hence the emitter-collector current. It is also possible to use the peculiar scattering rate of undoped (or ungated) graphene, which is totally suppressed due to phase space restrictions [8]. With the application of gate voltage one can easily tune the Fermi level through the electron density, so that the damping process via e-e or/and e-ph interaction can be activated and deactivated.

In conclusion, we have calculated the inelastic scattering rate $1/\tau$ and the inelastic mean free path l in graphene. We find that $\tau \sim 10^{-2} - 10^{-1} \text{ ps}$ and $l \sim 10 - 10^2 \text{ nm}$, with a finite step jump at 200 meV at the LO phonon energy. Our results have direct relevance to ballistic transport in graphene fast device structures.

This work is supported by US-ONR, NRI-SWAN and NSF-NRI.

-
- [1] See, for example, the Graphene special issue of Solid State Communications, vol. **143**, p.1-123 (2007), edited by S. Das Sarma, A.K. Geim, P. Kim, and A.H. MacDonald.
- [2] K. S. Novoselov *et al.*, Science **306**, 666 (2004); Y.-W. Tan *et al.*, Phys. Rev. Lett. **99** 246803 (2007); J.-H. Chen *et al.*, Nat. Phys. **4**, 377 (2008).
- [3] M.C. Lemme *et al.*, IEEE Electron Device Lett. **28**, 282 (2007); J.R. Williams, L. DiCarlo and C.M. Marcus, Science **317**, 638 (2007); G. Liang *et al.*, IEEE Trans. Electron Devices **54**, 657 (2007); G. Gu *et al.*, Appl. Phys. Lett. **90**, 253507 (2007).
- [4] E. H. Hwang, S. Adam and S. Das Sarma, Phys. Rev. Lett. **98**, 186806 (2007); S. Adam and S. Das Sarma, Solid State Commun. **146** 356 (2008).
- [5] A.C. Ferrari *et al.*, Phys. Rev. Lett. **97**, 187401 (2006).
- [6] J. H. Chen *et al.*, Nat. Nanotech. **3**, 206 (2008); S. V. Morozov, K. S. Novoselov *et al.*, Phys. Rev. Lett. **100**, 016602 (2008); E. H. Hwang and S. Das Sarma, Phys. Rev. B **77**, 115449 (2008)
- [7] W.-K. Tse and S. Das Sarma, Phys. Rev. Lett. **99**, 236802 (2007).
- [8] S. Das Sarma, E. H. Hwang, and W. K. Tse, Phys. Rev. B **75**, 121406 (2007).

- [9] T. Ando, J. Phys. Soc. Jpn. **75**, 124701 (2006).
- [10] E. H. Hwang and S. Das Sarma, Phys. Rev. B **75**, 205418 (2007).
- [11] R. Jalabert and S. Das Sarma, Phys. Rev. B **40**, 9723 (1989).
- [12] E. H. Hwang and S. Das Sarma, Phys. Rev. B **77**, 081412(R) (2008); E. H. Hwang, B. Y. K. Hu, and S. Das Sarma, Phys. Rev. B **76**, 115434 (2007); Physica E **40**, 1653 (2008).
- [13] J. M. Dawlaty *et al.*, Appl. Phys. Lett. **92**, 042116 (2008).
- [14] A. Palevski *et al.*, Phys. Rev. Lett **62**, 1776 (1989); T. Sakamoto *et al.*, Appl. Phys. Lett. **76**, 2618 (2000).